Journal of Polymer Research (2018) 25: 136
https://doi.org/10.1007/s10965-018-1535-1

ORIGINAL PAPER

Design and formulation of polyurethane foam used for porous alumina ceramics

Xinyue Tang[1] · Zaijuan Zhang[2] · Xiaoyan Zhang[2] · Wenlong Huo[2] · Jingjing Liu[2] · Shu Yan[2] · Jinlong Yang[1,2]

Received: 3 August 2017 / Accepted: 1 May 2018 / Published online: 8 May 2018

Abstract

The present work studied a simple direct foaming method for preparation of porous alumina ceramics by expansion of a ceramic suspension based on polyurethane (PU) foam system. The effects of polyurethane formulas including catalyst composition, blowing agent content, NCO index and solid content on the samples properties were investigated. The results showed that the homogeneity, porosity and mechanical properties are various for different formulas. The dried green bodies showed diametrical compressive strength in the range of 0.39–1.25 MPa and were amenable to machining operations such as milling, drilling and lathing. Meanwhile, PU formulas play an important role in the microstructures and mechanical properties of green bodies and sintered ceramic foams. Pyrolytic removal of polyurethane skeleton followed by sintering at 1550 °C produced alumina bodies with open cell porosity 54–75% and diametrical compressive strength 1.39–28.47 MPa. Microstructure showed both large (200–300 μm) and small (50–100 μm) pores all with various sizes of windows. Based on the optimization of polyurethane formulation, the porous alumina foam with porosity of 64% and compressive strength of 25.26 MPa was prepared. This polyurethane foam system is easily available and low-cost, which could be widely applied in preparation of other porous ceramics, such as ZrO_2, SiO_2, etc.

Keywords Polyurethane · Foam · Porous ceramics · Direct foaming method

Introduction

Generally, ceramic foams could be divided into two categories based on their microstructure, open-cell and closed-cell, which make them suitable for various applications. Open-cell ceramics are used as molten metal filtration, hot gas filtration, organism carrier in sewage disposal, acoustic material, aerospace, nuclear waste storage, porous electrodes, solar absorber and so forth [1–6]. Closed-cell ceramic foams can be applied to heat insulator material such as sintering furnace lining, protection project such as shock-absorbent and explosive attenuation materials. Furthermore, porous ceramics can also be used for biomedical materials, like artificial bone [7–9], transportation fuel cell and wearable composite materials [10].

Over the past few years, there has been an increasing interest in developing new routes for preparation of porous ceramics due to their wide applications, including sacrificial template method, polymer foam replication method and direct foaming method. The latter two methods are often designed to be used in conjunction with the polymer, such as polyurethane.

Polymer foam replication method, patented by Schwartzwalder and Somers in 1963 [11–13], is often made by immersing polyurethane foams with ceramic slurry, removing excess slurry from sponge and then burning out the PU templet [14–16]. It is a simple, low-cost and versatile way for producing ceramic foams with a 3D interconnected pore structure. However, the most significant barrier faced by this method is that the resulting foams consist of hollow struts with sharp edges and central hole, due to the burning out of the polymeric template [17, 18], Besides, its technological process is complex. The direct foaming method usually includes

✉ Zaijuan Zhang
zhangzaijuan1009@126.com

✉ Jinlong Yang
jlyang@mail.tsinghua.edu.cn

[1] School of Materials Science and Engineering, Dalian Jiaotong University, Dalian 116028, People's Republic of China

[2] State Key Laboratory of New Ceramics and Fine Processing, School of Materials Science and Engineering, Tsinghua University, Beijing 100084, People's Republic of China

particle-stabilized foams, surfactant-stabilized foams and in-situ polymer blowing method [19–21]. Among them, the in-situ polymer blowing method was firstly patented by Wood in 1974 [22] and a two-part PU system included polyol and isocyanate was often used [23–27]. The method is made by dispersing the ceramic powders to PU systems, foaming after suitable stirring, and then getting ceramic foams by removing the organics. The direct foaming method with polyurethane system has several distinct advantages over other methods. (1) The green body has high strength due to the existence of polyurethane skeleton. (2) It has no specific requirement for ceramic powders, which means it is suitable for any system. (3) The period of cure and produce is short.

Although in-situ polymer blowing method of polyurethane system has been used to prepare the porous ceramics, few research about the PU formulation design was studied, which plays a determining role in the properties of porous ceramics. There are many PU foam systems, but not all systems are suitable for the preparation of porous ceramics. In this work, we prepared the porous alumina ceramics with different polyurethane formulas and discussed the impacts on the microstructures and mechanical properties, and then obtained the optimum polyurethane formula can be applied in the fabrication of several ceramics.

Experimental

Materials

Commercially α-alumina (CT3000SG, D50 = 0.35 μm, Almatis, Ludwigshafen, Germany) was used as ceramic powder. Polymerized Diphenyl-methane-diisocyanate (PM-200, Wanhua chemical Co., LTD, NCO equivalent: 7.44 mmol/g, $f = 2.65$), and polyether polyol (R2305, Wanhua chemical Co., LTD, $M_n = 500$ g/mol, OH equivalent: 5.91 mmol/g) were designed to form ceramic loaded polyurethane foams. The chemical structure of the polyether polyol was shown as Fig. 1. Silicone oil was used as foam stabilizer. 33 wt% triethylenediamine with polyethylene glycol ($M_n = 200$ g/mol) as solvent (A33) and dibutyltin dilaurate (T-12) were used as catalyst. Distilled water was added as a foaming agent.

Characterization methods

The total porosity of sintered foams was determined from bulk density to theoretical density ratio:

$$P = (1 - D_b/D_t) \times 100\%$$

Here, P represents the total porosity of obtained foams, D_t and D_b represent the true density of alumina (3.97 g/cm^3) [28] and bulk density of ceramic foams respectively. The bulk densities are calculated from mass-to-volume ratio of ceramic foams.

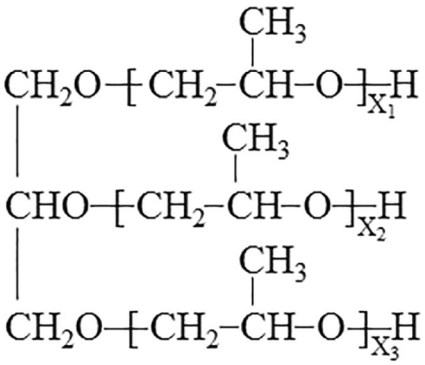

Fig. 1 Chemical structure of polyether polyol (R2305)

Thermal decomposition of PU was studied using TGA(TGA/DSC1SF/ 417–2, Mettler Toledo) employed a heat rate of 10 °C/min from room temperature to 600 °C in an air atmosphere (40 mL/min).

The microstructure of dried foams and sintered foams were characterized using scanning electron microscope (MERLIN VP Compact, Carl Zeiss, Jena, Germany) to investigate their morphology.

Compressive strength of sintered foams and green bodies was measured using a universal material testing machine (AG2000G, Shimadzu, Japan) with a loading rate of 1 mm/min. For each point, three samples were measured to obtain the average values and standard deviation of compressive strength.

Preparation of porous alumina ceramics

Figure 2 highlights the preparation process of porous alumina ceramics in this work. Firstly, a pre-calculated amount of alumina powder was added into the mixture of isocyanate, polyols and silicone oil with constant stirring at a speed of ~300 r/min, followed by adding 0.1 ~ 0.2 wt% catalyst based on the polyol. After stirring for some time, 0.6 ~ 1.2 wt% water was added to the system as a blowing agent with a rapid fully mixing (~700 r/min). Then the suspensions foamed and cured at room temperature to get a green body, which decomposed at 600 °C to remove the polyurethane thoroughly (Fig. 3). Finally, the sample was sintered at 1550 °C to obtain the porous alumina ceramics.

Results and discussion

Pyrolysis of alumina green body

Figure 3 shows the TGA diagram of loaded foams with 63 wt% solid content. In TGA curve of foams under low

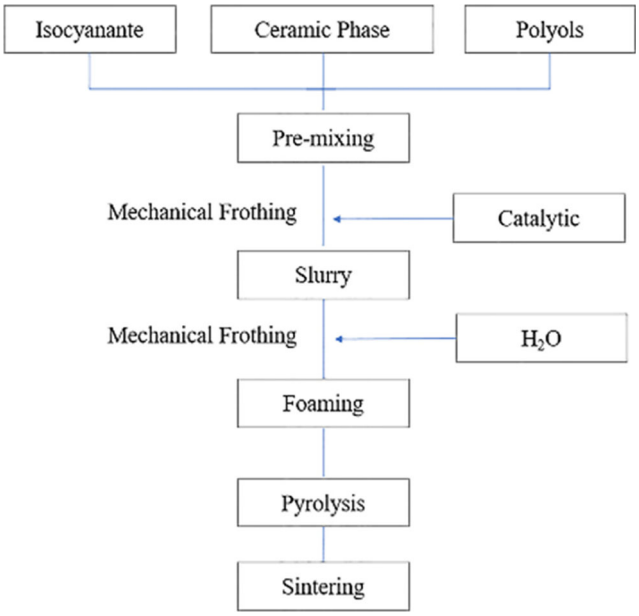

Fig. 2 Preparation process of porous alumina ceramics

temperature, three characteristic weight loss steps were observed. The first step started at 258 °C and ended at 318 °C with the weight loss of 20.0%, corresponding to the decomposition of urethane segment. The second stage involved the decomposition of the polyether skeleton between 318 and 450 °C with a weight loss of 4.0%. The third stage corresponding to the char residue was completed nearly at 600 °C with a weight loss of 13.0%. After the third stage of decomposition, the residue left behind is 63.0%, which was in agreement with the theoretical solid loading, and showed that the organic component was decomposed completely after 600 °C [29–32].

Effect of catalysts composition

The addition of catalyst actually accelerates the rate of reactions, and what's more, a balance between the gel reaction and the foaming reaction can be achieved by adjusting the catalyst composition [33]. The organotin-based catalyst, such as T-12, mainly accelerates the crosslinking reaction rate, on the contrary, amine catalyst, such as A33, plays more important role in the foaming reaction. The mixture of the two with appropriate proportion is often used as catalyst to keep the balance between crosslinking reaction (Eqs. 1 and 3) and foaming reaction (Eq. 2). In order to verify the proportion of the mixed catalyst, experiments have been carried out.

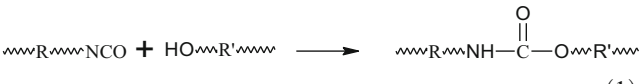

(1)

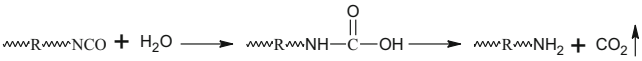

(2)

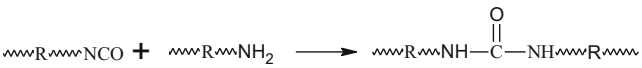

(3)

The structures of green bodies and sintered foams prepared with different proportion catalysts are shown in Figs. 4 and 5. In the green body prepared by only T-12, the pores exist obvious distortion (Fig. 4a), which lead to the pores of sintered alumina foams be destroyed severely

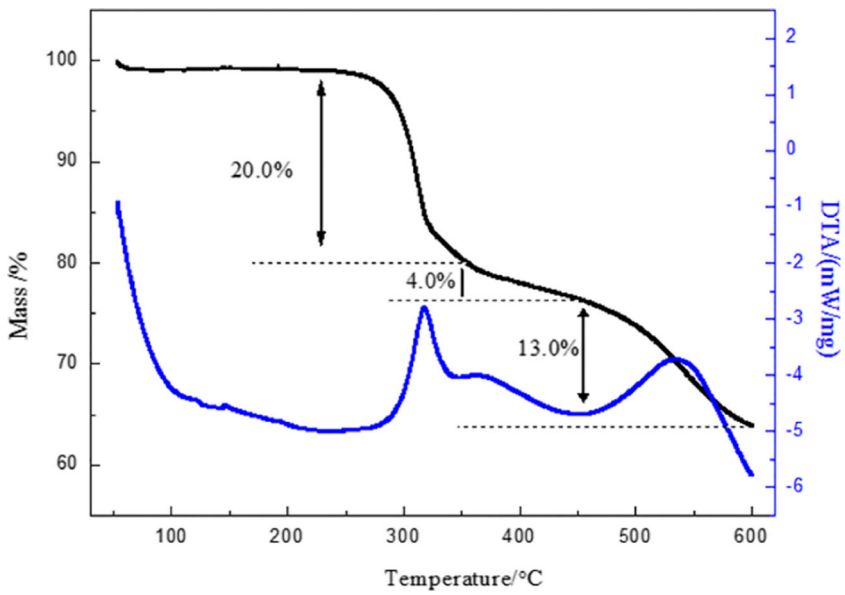

Fig. 3 TGA curves for alumina green body with 63 wt% solid content

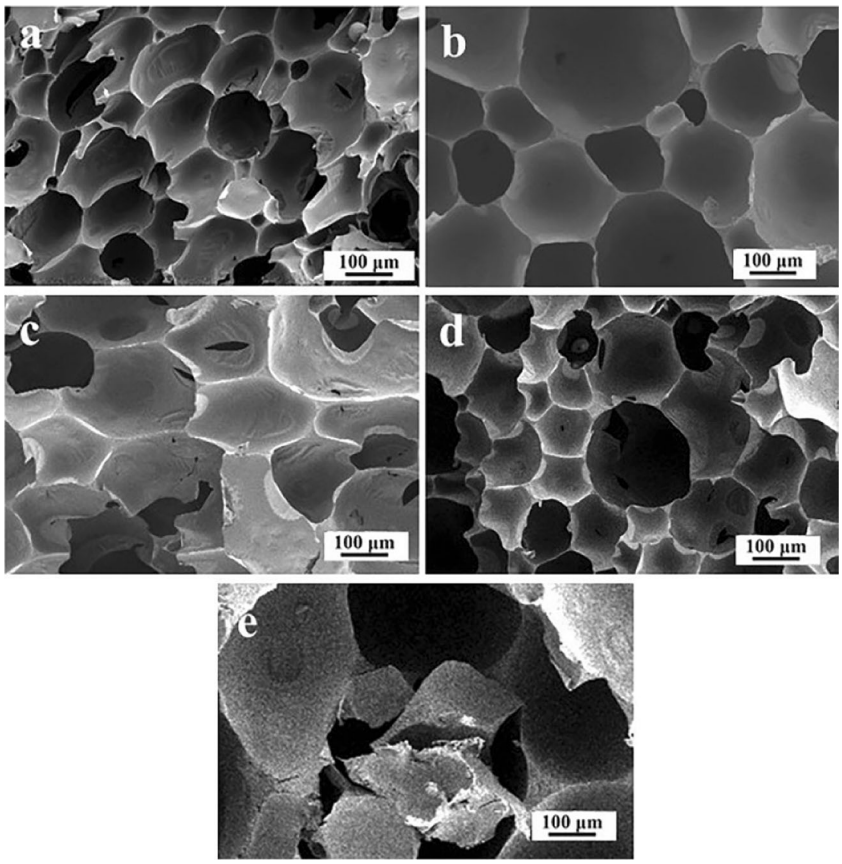

Fig. 4 SEM images of green bodies prepared with different proportion catalysts: **a** A33:T-12 = 0:1; **b** A33:T-12 = 1:3; **c** A33:T-12 = 1:1; **d** A33:T-12 = 3:1; **e** A33:T-12 = 1:0

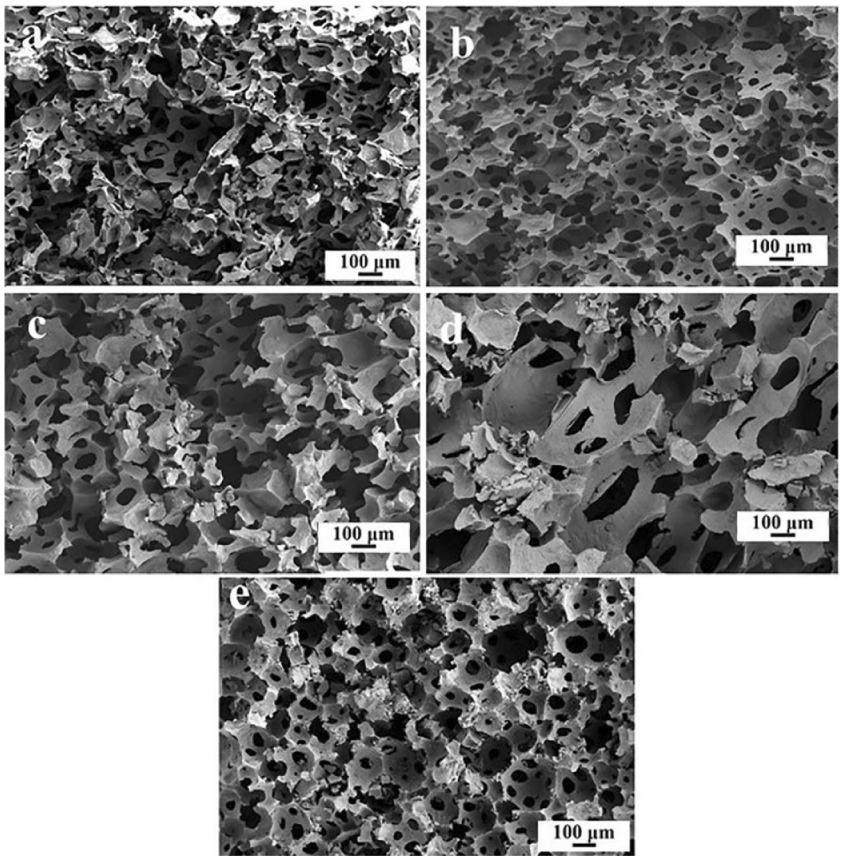

Fig. 5 SEM images of sintered alumina foams prepared with different proportion catalysts: **a** A33:T-12 = 0:1; **b** A33:T-12 = 1:3; **c** A33:T-12 = 1:1; **d** A33:T-12 = 3:1; **e** A33:T-12 = 1:0

Table 1 The properties of foams prepared with different proportion catalysts

Catalyst	Total porosity (%)	Green body compressive strength (MPa)	Sintered foam compressive strength (MPa)
A33:T-12 = 0:1	76	0.55 ± 0.06	6.89 ± 0.08
A33:T-12 = 1:3	64	0.67 ± 0.09	25.26 ± 0.01
A33:T-12 = 1:1	68	0.80 ± 0.11	19.78 ± 0.04
A33:T-12 = 3:1	76	1.05 ± 0.20	1.39 ± 0.08
A33:T-12 = 1:0	60	1.25 ± 0.06	–

(Fig. 5a). In this system, the crosslinking reaction rate is much higher than the foaming reaction and therefore the strength of bubble wall is so strong that the bubbles are difficult to grow. The green body has a lower mean pore size of 153.04 μm. When using A33 alone, a majority of pores burst and only a portion of the pore structure remain (Figs. 4e and 5e). The mean pore size of green body is 265.51 μm, which is obviously greater than the sample prepared by only T-12 because its crosslinking reaction is slower than the foaming reaction. The bubble wall strength is so weak that the CO_2 can easily broke through the walls leading to the green body be broken. Using either of the two catalysts alone cannot allow the crosslinking reaction and foaming reaction achieving a balance. Figures 4b–d and 5b–d show the cell size distributions and morphology of foams with the compound catalyst. When the ratio of A33 to T-12 is 1 to 3 (Fig. 4b), all pores of green body are complete without broken with the mean size of 249.22 μm and these pores remain intact after sintering (Fig. 5b). For the ratio is 1:3, two reactions can reach a balance and then obtain the porous ceramic foams with complete pore structure. When the ratio is 1:1 and 3:1 (Fig. 4c–d), the mean pore size are 346.22 μm and 194.55 μm respectively, just like the foam used A33 alone, the foaming reaction rate is so high that the bubbles get close to each other to form larger bubbles and even cause extrusion deformation and burst, which further leads to the pores in sintered foams be destroyed (Fig. 5c–d).

In addition, from Table 1 we can see that the compressive strength of sintered alumina foams has a significant improvement (25.26 MPa) when the mass ratio is 1:3, due to its intact pore structure. To illustrate, when using only A33 as catalyst, the sintered alumina foam is hollow because of its fragile skeleton.

Effect of water content

Using the catalyst ratio optimized above (A33:T-12 = 1:3), the effects of water content on the properties of Al_2O_3 porous ceramics are revealed. As water content increasing from 0.6 to 1.2% with an interval of 0.2%, the mean pore sizes of foams are 144.18, 249.22, 261.80 and 297.89 μm. The increase in the content of foaming agent increases the mean pore size. When the addition of water is too high (1.0 and 1.2%) or too low (0.6%), there is a macro-deformation in sintered foams as shown in Fig. 6. A typical microstructure of a fracture surface of green bodies and corresponding sintered foam is shown in Figs. 7 and 8 respectively. When the addition of water is 1.0% or 1.2%, the foaming reaction rate is so rapid that the surface tension of slurry cannot effectively curb CO_2 emissions, leading to the escape of gas and the burst of bubbles in green body like the Fig. 7c–d here. The distorted bubbles will further cause the broken of the pores in sintered ceramic foam, as shown in Fig. 8c–d. When adding 0.8% water, the sintered ceramics foam can hold its square shape without appreciable macroscopic deformation (Fig. 6b).

Table 2 shows the properties of porous ceramics prepared with different water content. From the data listed in Table 2, the increase of addition of water makes the larger stomatal aperture and higher porosity, which further leads to lower compressive strength of green bodies. As the water content increases from 0.6 to 1.2%, the compressive strength of sintered foams shows its maximum value, up to 25.26 MPa

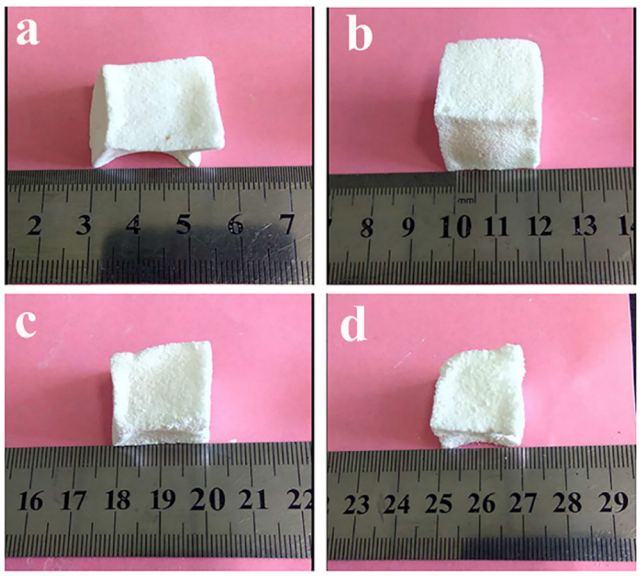

Fig. 6 Pictures of sintered foams with different water content: **a** 0.6 wt%; **b** 0.8 wt%; **c** 1.0 wt%; **d** 1.2 wt%

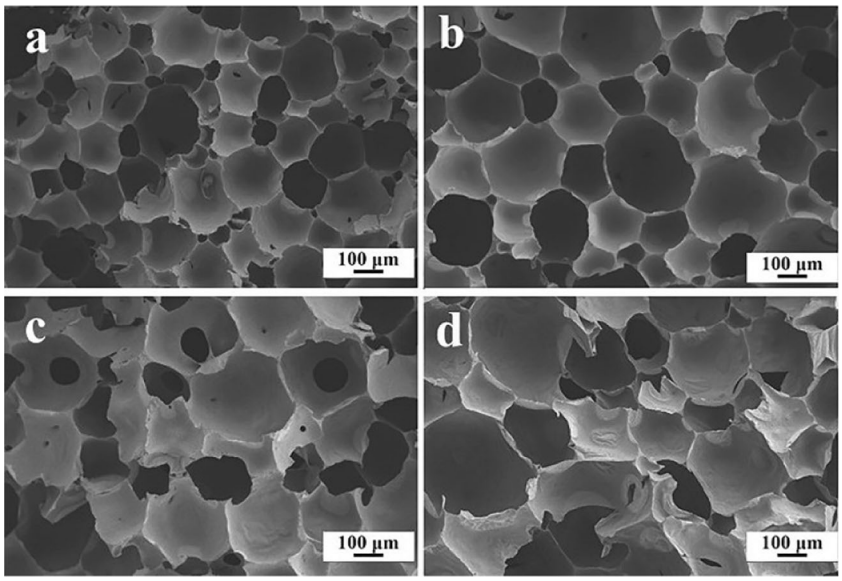

Fig. 7 SEM images of dried alumina foams with different water content: **a** 0.6 wt%; **b** 0.8 wt%; **c** 1.0 wt%; **d** 1.2 wt%

at 0.8%. When the additive amount of water is lower than 0.8 wt%, the faster crosslinking reaction rate would result in the rapid increase of the viscosity and cause the deformation and nonuniform of pores, leading to low compressive strength. When the additive amount of water is greater than 0.8 wt%, more uramido group is generated accompanying highly exothermic, which promotes the whole reaction reach the physical gel point quickly and induces the serious deformation (Fig. 8c–d).

Effect of NCO index

NCO index is the mole ratio of NCO to OH. In the process of reactions, PM200 is the main source of NCO, while raw materials with OH are R2305, foaming agent H_2O and polyethylene glycol which is solvent of catalytic A33. What is noteworthy is that the hydroxyl value of polyethylene glycol could be ignored due to its small amounts according to our early results. For example, when the NCO/OH index is 1.10 and the mass ratio of A33 to T-12 is 1:3, the dose of PM200 reacted with the polyethylene glycol is just 0.00825 wt% based on the slurry.

The microstructure of sintered ceramics prepared with different NCO index is shown in Fig. 9. According to the SEM images, NCO index plays an important role in the pores morphology and uniformity. When the NCO index is low (like 1.0 and 1.05), the absence of NCO functional groups will cause crosslinking reaction incomplete and

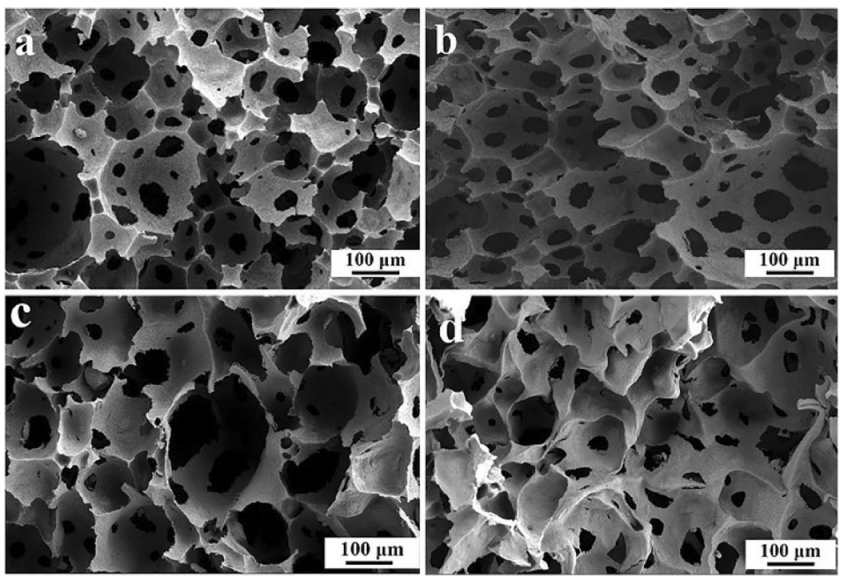

Fig. 8 SEM images of sintered foams with different water content: **a** 0.6 wt%; **b** 0.8 wt%; **c** 1.0 wt%; **d** 1.2 wt%

Table 2 The properties of foams prepared with different water content

Water (%)	Apparent porosity (%)	Total porosity (%)	Green body compressive strength (MPa)	Sintered foam compressive strength (MPa)
0.6	64	67	0.75 ± 0.04	6.36 ± 0.03
0.8	62	64	0.67 ± 0.09	25.26 ± 0.01
1.0	73	73	0.55 ± 0.01	5.16 ± 0.04
1.2	77	79	0.39 ± 0.09	3.49 ± 0.08

the reticular skeleton distorted (Fig. 9a–b). On the contrary, too-high NCO index (like 1.15) leads to a higher reaction rate of cross-linking reaction than the generation of CO_2. The excess isocyanate is easy to react with uramido (Eq. 4) and carbamate (Eq. 5) generating biuret and allophanate respectively [34].

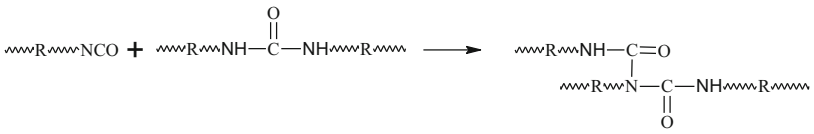

(4)

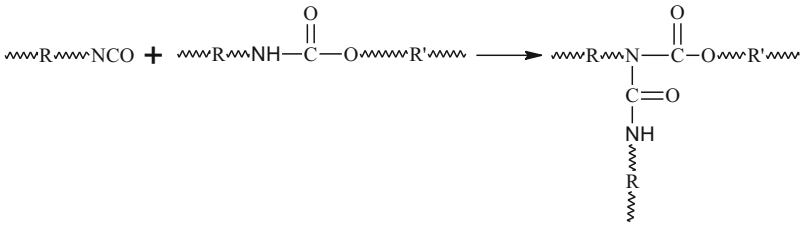

(5)

The two side reactions will easily cause the pores shrink and deformation. When the NCO index is 1.10, crosslinking reaction and foaming reaction can reach an equilibrium and porous alumina ceramics with complete pores can be obtained. Table 3 shows the properties of porous ceramics prepared with different NCO index. When the NCO index is 1.1, the

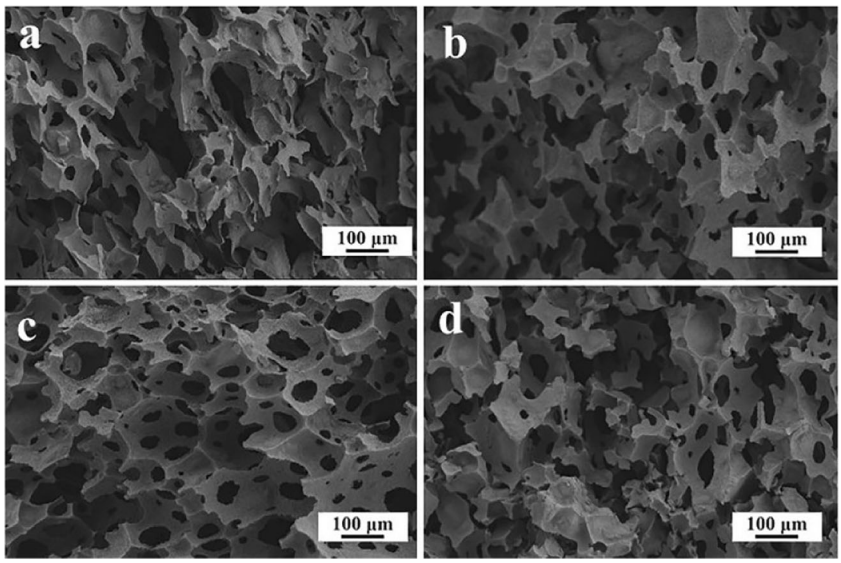

Fig. 9 SEM images of sintered alumina foams prepared with different NCO index: **a** 1.0; **b** 1.05; **c** 1.10; **d** 1.15

Table 3 The properties of foams prepared with different NCO index

NCO index	Apparent porosity (%)	Total porosity (%)	Green body compressive strength (MPa)	Sintered foam compressive strength (MPa)
1.00	57	59	0.40 ± 0.03	22.70 ± 0.04
1.05	56	58	0.44 ± 0.02	28.47 ± 0.02
1.10	62	64	0.67 ± 0.09	25.26 ± 0.01
1.15	62	66	0.90 ± 0.04	20.03 ± 0.06

sample has the complete and uniform pore structure with 64% porosity and 25.26 MPa sintered foam compressive strength.

Effect of solid content

Figure 10 shows SEM microstructure of the green bodies and sintered foams with different additive amount of alumina powder. When the solid contents are 63, 59 and 55%, the mean pore sizes of green bodies are 249.22, 153.62 and 200.53 μm respectively. All green bodies have regular pore morphology due to the same optimized formulation of polyurethane matrix previously in this paper (Fig. 10a–c). However, when the solid content is low, the ceramic powder cannot distribute on the walls of the pores uniformly and completely. With the removal of polyurethane skeleton going on, the sintered foams appear to be cracked because of the mechanical property of sintered foams is too poor to keep their original shape (Fig. 10e–f). On the other hand, when the solid content is higher than 63%, the viscosity of the system is too high to make the blowing agent uniformly disperse in the mixtures, leading to difficulties in foaming. The porosity and compressive strength of alumina foams with various solid contents are tested in Table 4. With the increase of solid content, the porosity increases and the compressive strength decreases. As we know, when the solid content is low (below 63%), the viscosity of the mixture is so low that the gas diffusion resistance during the foaming process decreases. With porosity of sintered alumina foams increasing from 64 to 73%, the compressive strength decreases from 25.26 to 4.02 MPa accordingly. When the content of solid is up to 63%, it displays the best mechanical properties.

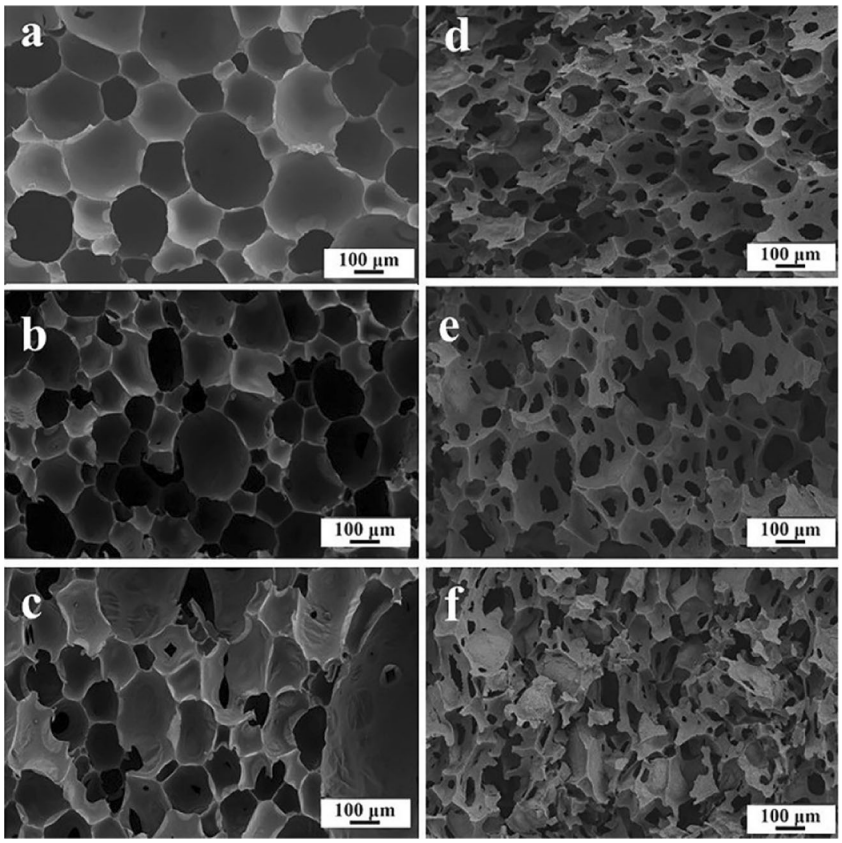

Fig. 10 SEM images of green bodies (**a** 63%; **b** 59%; **c** 55%) and sintered alumina foams (**d** 63%; **e** 59%; **f** 55%) with different solid content

Table 4 The properties of sintered foams prepared with different solid content

Solid content (wt%)	Total porosity (%)	Compressive strength (MPa)
63	64	25.26 ± 0.01
59	69	6.56 ± 0.02
55	73	4.02 ± 0.01

Conclusion

In this work, the polyurethane foam system was used to prepare the porous alumina ceramics. The in-situ polymerization of polyol and isocyanate leads to cross-linking reactions and rapid solidification, therefore, the strength of obtained green body is so high to 1.29 MPa that can withstand machining. By comparing the microstructures and compressive strength of samples, the optimum polyurethane formulation was achieved, there as follows: the mass ratio of A33 to T-12 is 1:3, the amount of water is 0.8 wt%, NCO index is 1.10 and solid content is 63 wt%. Using the best formula, porous alumina ceramics with intact pore structure were prepared. What should be of concern is that the optimizing polyurethane formulation can be widely applied to produce a series of porous ceramics like ZrO_2, CeO_2 and TiO_2, and so on.

Funding This project was funded by China Postdoctoral Science Foundation (Grant no.2017 M610085), National Natural Science Foundation of China (NSFC, No. 51702184) and National Natural Science Foundation of China (NSFC, No. 51572140).

References

1. Mey-Cloutier S, Caliot C, Kribus A, Gray Y, Flamant G (2016) Experimental study of ceramic foams used as high temperature volumetric solar absorber. Sol Energy 136:226–235
2. Studart AR, Gonzenbach UT, Tervoort E, Gauckler LJ (2006) Processing routes to macroporous ceramics: a review. J Am Ceram Soc 89(6):1771–1789
3. Wang S, Zhou M, Zeng L, Dai W (2016) Investigation on the preparation and properties of reticulate porous ceramic for organism carrier in sewage disposal. J Ceram Process Res 17(10):1095–1099
4. Zhang Y, He F, Xia S, Kong L, Xu D, Wu Z (2014) Adsorption of sediment phosphorus by porous ceramic filter media coated with nano-titanium dioxide film. Ecol Eng 64:186–1925
5. Mardkhe MK, Huang B, Bartholomew CH, Alam TM, Woodfield BF (2016) Synthesis and characterization of silica doped alumina catalyst support with superior thermal stability and unique pore properties. J Porous Mater 23(2):475–487
6. Moon Y-W, Choi I-J, Koh Y-H, Kim H-E (2015) Porous alumina ceramic scaffolds with biomimetic macro/micro-porous structure using three-dimensional (3-D) ceramic/camphene-based extrusion. Ceram Int 41(9):12371–12377
7. Chang BS, Lee CK, Hong KS, Youn HJ, Ryu HS, Chung SS, Park KW (2000) Osteoconduction at porous hydroxyapatite with various pore configurations. Biomaterials 21(12):1291–1298
8. Klawitter J, Hulbert S (1971) Application of porous ceramics for the attachment of load bearing internal orthopedic applications. J Biomed Mater Res A 5(6):161–229
9. Better H, Osiroff R, Gross Y (2012) Ceramic foam artificial bone. U.S. Patent Application No. 13/305,301
10. Wachsman ED, Bishop SR (2012) Porous ceramic molten metal composite solid oxide fuel cell anode. U.S. Patent Application No. 13/416,417
11. Karl S, Somers AV (1963) Method of making porous ceramic articles. U.S. Patent No. 3,090,094
12. Jo IH, Shin KH, Soon YM, Koh YH, Lee JH, Kim HE (2009) Highly porous hydroxyapatite scaffolds with elongated pores using stretched polymeric sponges as novel template. Mater Lett 63(20):1702–1704
13. In-Kook J, Song JH, Won-Young C, Young-Hag K, Hyoun-Ee K, Hae-Won K (2007) Porous hydroxyapatite scaffolds coated with bioactive apatite-Wollastonite glass-ceramics. J Am Ceram Soc 90(9):2703–2708
14. Bao X, Nangrejo MR, Edirisinghe MJ (2000) Preparation of silicon carbide foams using polymeric precursor solutions. J Mater Sci 35(17):4365–4372
15. Pan JM, Yan XH, Cheng XN, Lu QB, Wang MS, Zhang CH (2012) Preparation of SiC nanowires-filled cellular SiCO ceramics from polymeric precursor. Ceram Int 38(8):6823–6829
16. Sepulveda P, Binner JGP (1999) Processing of cellular ceramics by foaming and in situ polymerisation of organic monomers. J Eur Ceram Soc 19(12):2059–2066
17. Oliveira FAC, Dias S, Vaz MF, Fernandes JC (2006) Behaviour of open-cell cordierite foams under compression. J Eur Ceram Soc 26(1–2):179–186
18. Jana P, Zera E, Sorarù GD (2016) Processing of preceramic polymer to low density silicon carbide foam. Mater Des 116(16):278–306
19. Sepulveda P, Ortega FS, Innocentini MDM, Pandolfelli VC (2000) Properties of highly porous hydroxyapatite obtained by the gelcasting of foams. J Am Ceram Soc 83(12):3021–3024
20. Sepulveda P (1997) Gelcasting foams for porous ceramics. Am Ceram Soc Bull 76(10)
21. Wang M, Du H, Guo A, Hao R, Hou Z (2012) Microstructure control in ceramic foams via mixed cationic/anionic surfactant. Mater Lett 88(88):97–100
22. Frisch K, Wood L, Messina P (1974) Method of prepairing porous ceramic structures by firing a polyurethane foam that is impregnated with inorganic material. U.S. Patent No. 3,833,386
23. Prabhakaran K, Melkeri A, Gokhale NM, Sharma SC (2007) Preparation of macroporous alumina ceramics using wheat particles as gelling and pore forming agent. Ceram Int 33(1):77–81
24. Powell SJ, Evans JRG (1995) The structure of ceramic foams prepared from polyurethane-ceramic suspensions. Mater Manuf Process 10(4):757–771
25. Colombo P, Griffoni M, Modesti M (1998) Ceramic foams from a preceramic polymer and polyurethanes: preparation and morphological investigations. J Sol-Gel Sci Technol 13(1):195–199
26. Neumann B, Elkins TW, Dreher W, Hagelinweaver H, Nino JC, Bäumer M (2012) Enhanced catalytic methane coupling using novel ceramic foams with bimodal porosity. Cat Sci Technol 3(1):89–93
27. Zhai T, Li D, Fei G, Xia H (2015) Piezoresistive and compression resistance relaxation behavior of water blown carbon nanotube/polyurethane composite foam. Compos A: Appl Sci Manuf 72:108–114
28. Chuanuwatanakul C, Tallon C, Dunstan DE, Franks GV (2011) Controlling the microstructure of ceramic particle stabilized foams:

influence of contact angle and particle aggregation. Soft Matter 7(24):11464–11474
29. Jiao L, Xiao H, Wang Q, Sun J (2013) Thermal degradation characteristics of rigid polyurethane foam and the volatile products analysis with TG-FTIR-MS. Polym Degrad Stab 98(12):2687–2696
30. Zhang Y, Xia Z, Huang H, Chen H (2009) Thermal degradation of polyurethane based on IPDI. J Anal Appl Pyrolysis 84(1):89–94
31. Gupta T, Adhikari B (2003) Thermal degradation and stability of HTPB-based polyurethane and polyurethaneureas. Thermochim Acta 402(1–2):169–181
32. Tien Y, Wei KH (2002) The effect of nano-sized silicate layers from montmorillonite on glass transition, dynamic mechanical, and thermal degradation properties of segmented polyurethane. J Appl Polym Sci 86(7):1741–1748
33. Thirumal M, Khastgir D, Singha NK, Manjunath B, Naik Y (2008) Effect of foam density on the properties of water blown rigid polyurethane foam. J Appl Polym Sci 108(3):1810–1817
34. Kwon OJ, Yang SR, Kim DH, Park JS (2007) Characterization of polyurethane foam prepared by using starch as polyol. J Appl Polym Sci 103(3):1544–1553